Eur Biophys J (1984) 11:111–115

European Biophysics Journal

Stimulus coding in crayfish antennal mechanoreceptors estimated by noise analysis

Y. Ebina[1] and J. Tautz*[2]

[1] Department of Electrical Engineering, Yamaguchi University, Ube-shi, 755 Japan
[2] Fakultät für Biologie, Universität Konstanz, Postfach 55 60, D-7750 Konstanz, Federal Republic of Germany

Received May 9, 1984/Accepted June 27, 1984

Abstract. Two different kinds of mechanoreceptive hairs (smooth and feathered) on the second antennae of the freshwater crayfish, *Orconectes virilis,* have been investigated for their stimulus coding properties. These mechanoreceptors show a great deal of non-linear behaviour both in threshold and in directionality. An effective approach for the investigation of such systems is noise analysis in the frequency domain. This method has been used here to calculate zero-, first- and second-order kernels. Sensory cells reveal different first- and second-order kernels, depending on which type of hair is being stimulated. The first-order kernel has a pronounced peak in the frequency response at 110 Hz if a feathered hair is stimulated and at 60 Hz if a smooth hair is stimulated. The second-order kernel shows a number of pronounced peaks in the frequency response between 40 and 110 Hz, but only if a feathered hair is stimulated. Smooth hair stimulation results in less sharp peaks but in higher gain for the same range of stimulus frequencies.

Key words: Stimulus coding, mechanoreceptor, crayfish, noise analysis

Introduction

The flagellum of the second antennae of freshwater crayfish possesses two classes of mechanoreceptive hairs, smooth and feathered. Electron microscopical investigation showed that only smooth hairs, not feathered hairs, are innervated (Bender et al. 1984). However, sensory cells that innervate smooth hairs can be stimulated not only directly, by moving the smooth hairs, but also indirectly, by moving feathered hairs. This results in two different threshold curves for impulse initiation in this sensory cell (Tautz et al. 1981). This threshold difference presumably results from different mechanical coupling between the two hair types and the transducing sensory receptor. Zero-, first-, and second-order kernels were calculated from noise analysis (see e.g., French 1976) in order to estimate the frequency characteristics of this coupling. This method is superior to the popular analysis using pure sine waves because no assumptions about the degree of linearity of the system are necessary. Furthermore, data collection by noise analysis is much less time-consuming than by sinusoidal stimulation.

Materials and methods

A. Stimulation and recording

Five mechanosensory cells on the flagellum of the second antennae of the crayfish, *Orconectes virilis,* were investigated. Action potentials of single sensory cells, evoked by hair displacement, were recorded extracellularly as described previously (Tautz et al. 1981). For mechanical stimulation single sensory hairs were directly coupled to a loudspeaker which moved the hair in a direction parallel to the long axis of the flagellum. The average stimulus intensity was above the threshold for impulse initiation in the sensory cells. The stimulus was registered by a calibrated photo-diode, the linearity of which was confirmed by microscopically measuring the displacement of a fixed point on the hair. The stimulus approximated band-limited, Gaussian white noise and was obtained in the following way. Broad-band, high-frequency noise (high cut off: 5 KHz) from a noise generator was recorded on tape and played back at a reduced speed in order to shift the frequency range to low frequencies. This signal was used to drive the VCA (voltage controlled amplitude) input of a function generator which produced rectangular pulses of 4 ms duration at 4-ms intervals, the

* To whom offprint requests should be sent

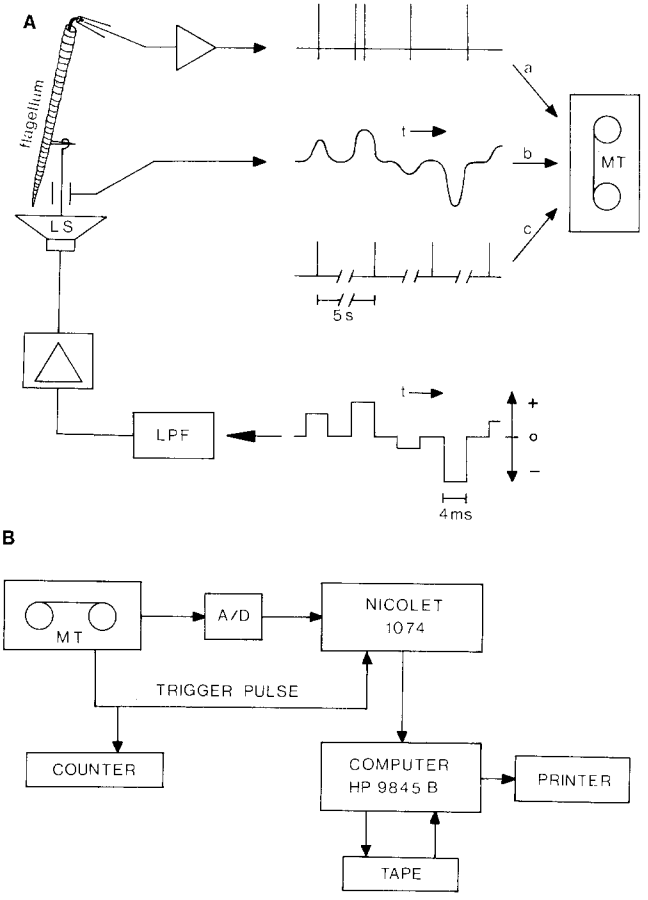

Fig. 1. A Scheme for the stimulation and recording procedure. *a* response (action potentials) of a sensory cell, *b* time course of the stimulus measured by a photo-diode, *c* trigger signal. *LPF* = low pass filter, *LS* = loudspeaker, *MT* = magnetic tape. **B** Diagram showing system used for data analysis. A/D = analog digital converter (used only for the stimulus analysis, omitted for response data analysis), *MT* = magnetic tape

amplitude of which was modulated around zero by the noise input. The output of the function generator was filtered through a low-pass filter (upper cut-off frequency: 300 Hz) and fed into a power amplifier which drove the loudspeaker. The monitored noise signal had a sharp decrease in its power spectrum above 125 Hz (Fig. 2). For computer analysis, the output of the photo-diode, the response of the sensory cell and a trigger signal (5-s intervals) were recorded on magnetic tape (Fig. 1A). All experiments were done at room temperature.

B. Data collection

The recorded time course of the stimulus [$X(t)$] was digitized with an analog to digital converter (Nicolet 1074) and fed into a computer (Hewlett-Packard 9845B) for analysis (Fig. 1B). A segment of data

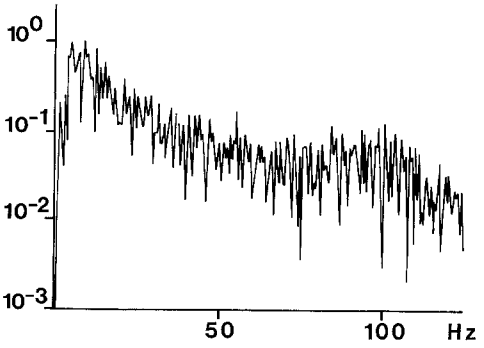

Fig. 2. Amplitude spectrum of the noise stimulus normalized to the maximum amplitude

included 2,048 sampling points in 8.192 s. The segment had to be divided into eight or four data blocks because of the speed of the fast Fourier transform (FFT) in the HP 9845B. The number of Fourier components (N) was therefore 256 or 512. Six segments were evaluated for each sensory cell, i.e., an experiment lasted about 48 s.

The responses (sensory cell impulses) were processed by counting the impulses in 2-ms bins and multiplying by a convolution function [$\sin(A)/A$, $A = \pi fT$, $f_{max} = 120$ Hz, see also French and Holden 1971]. The convoluted number of impulses [$Y(t)$] was used for FFT with a sampling time of 4 ms.

C. Data analysis

The kernels were calculated in the frequency domain because first-order kernels can be directly compared with Bode plots (amplitude and phase spectra) and because Fourier-transformed components are less sensitive to time shifts (French 1976; French and Wong 1977; Marmarelis and Marmarelis 1978). The practical expressions for the kernels are given by French (1976) as follows:

$$K_0 = Y(0) \tag{1}$$

$$K_1(\omega) = \{Y(\omega)\bar{X}(\omega)\} / \{X(\omega)\bar{X}(\omega)\} \tag{2}$$

$$K_2(\omega, \eta) = \{Y(\omega + \eta)\bar{X}(\omega)\bar{X}(\eta)\}/ 2\{X(\omega)\ \bar{X}(\omega)\}\{X(\eta)\bar{X}(\eta)\},\ \omega + \eta \neq 0, \tag{3}$$

where $X(\omega)$ is the Fourier transform of the stimulus, $X(t)$ and $Y(\omega)$ is that of the response of the sensory cell, $Y(t)$. $\bar{X}(\omega)$ means the complex conjugate of $X(\omega)$, $\{\ldots\}$ stands for an ensemble average. In Eq. (3), an additional DC term $(K_0 \cdot \delta\ (\omega + \eta)/2A)$ is neglected (for justification see French 1976).

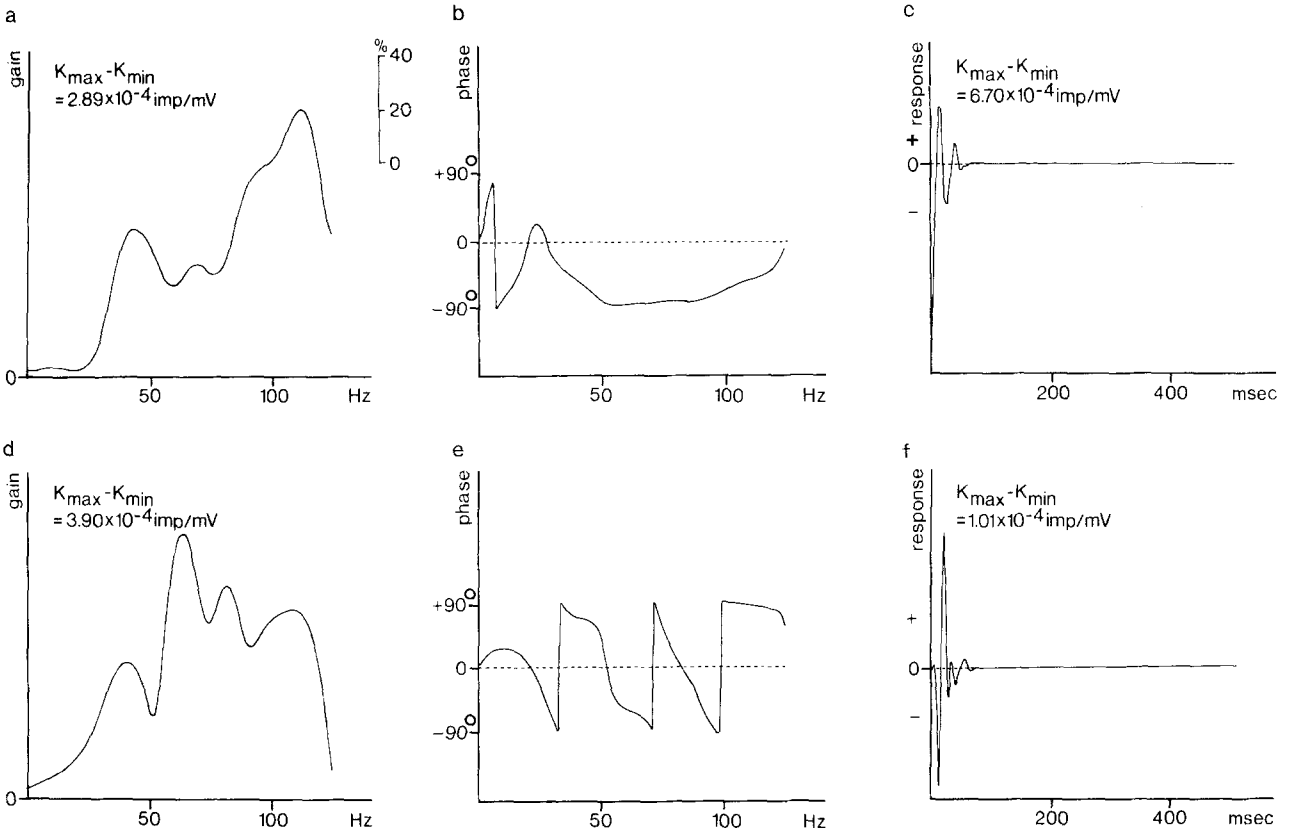

Fig. 3a–f. First-order kernels for a feathered hair (**a**: frequency response, **b**: phase curve, **c**: inverse frequency response – all three plots were obtained from the same set of data) and for a smooth hair (**d**: frequency response, **e**: phase curve, **f**: inverse frequency response – all three plots were obtained from the same set of data). The ordinate represents percentages of $K_{max}-K_{min}$, the overall size of a curve

Results

Zero-order kernel

Using a mean value of $Y(\omega = 0)$, zero-order kernels range from 1 to 10 (impulses/s) for both kinds of hairs. These values represent the range of activity of sensory cells when the stimulus frequency is zero.

First-order kernel

The first-order kernel is given by Eq. (2). If $K_1(\omega)$ is plotted versus the frequency, f or ω (= 2πf), the resulting curves show multiple peaks typical of impulse data, even when n = 512 (over 24 data blocks) or 256 (over 48 data blocks). However, the envelopes are similar in all cases. Accepting some loss of frequency resolution, two different methods of curve smoothing were used. In the first method, mean values of four or eight neighbouring frequency components were used to calculate the ensemble average. Thus $K_1(\omega)$ is expressed by 64 components. In the second method, a three-point averaging method, the amplitude at every frequency ω_i was replaced by $\omega_{i-1}/4 + \omega_{i+1}/4 + \omega_i/2$. This method keeps the original frequency components unchanged and gives a smoother curve for the same axis. The second method was tried by averaging 2, 8, 40, 100, and 200 times. Averaging more than 40 times produced curves that resemble those resulting from Method 1. Figure 3a and d give results for the two types of hair (Fig. 3a: feathered hairs, Fig. 3d: smooth hairs) obtained by averaging 100 times using Method 2.

In comparing these two curves, it is obvious that both types of hair have different ranges of optimal frequency. Feathered hairs respond maximally to sine waves around 110 Hz, smooth hairs around 60 Hz. From these two curves the phase angles can be calculated by taking the principal values of $\tan^{-1}$ [imaginary $K_1(\omega)$/real $K_1(\omega)$]. The phase curve for feathered hairs (Fig. 3b) shows abrupt changes only below 20 Hz, whereas the phase curve for smooth hairs (Fig. 3e) shows such discontinuities over the whole frequency range. The data of Fig. 3a and d can also be used to calculate an inverse FFT. The results are given in Fig. 3c and f. A damped oscillation results for both types of hair.

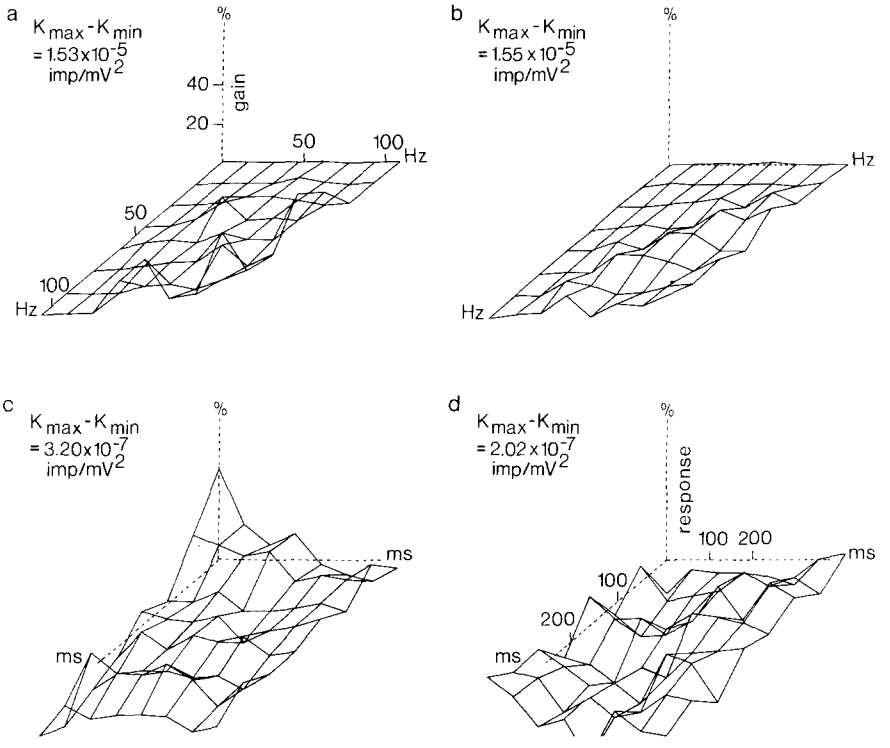

Fig. 4a–d. Second-order kernels for a feathered hair (**a:** two-dimensional frequency response, **c:** its inverse – same axis as **d**) and a smooth hair (**b:** two-dimensional frequency response – same axis as **a; d:** its inverse). Interpret K_{max}-K_{min} as in Fig. 3

Second-order kernel

Second-order kernels $K_2(\omega,\eta)$ were calculated by Eq. (3) using the first smoothing method. This calculation was done with one eights data reduction, resulting in 32 frequency components. The high frequency part of $Y(\omega + \eta)$ was set to zero above ω_{max} (for explanation see French and Wong 1977). Figure 4a (feathered hairs) and b (smooth hairs) show the gain of $K_2(\omega,\eta)$ obtained from the same data (over 48 s) that were used to compute the curves in Fig. 3a and d, respectively. For the sake of clarity, the curves were only plotted for some values of $K_2(\omega,\eta)$. Figure 4c and d give the two-dimensional inverse FFT of the curves in Fig. 4a and b, respectively.

Discussion

Bode-plots (amplitude and phase spectra of input/output relation) are commonly used to determine the transfer characteristics of a receptor. This approach is justified only in linear systems. If the linearity of the system under investigation is uncertain, the noise approach used in the present study will give a more realistic description of the transfer characteristics of the system. Over a certain range of stimulus intensity and frequency, however, a receptor may indeed behave like a linear system (e.g., Chapman and Smith 1963). For the linear range of a receptor, Bode-plots and the first-order kernels are identical. Thus comparison between a Bode-plot and a first-order kernel calculated for the same system can tell a posteriori if an assumption of linearity is justified.

The use of the frequency domain approach described by French and Butz (1973) and French (1976) in analysing non-linear systems has a number of advantages over the Laguerre function method proposed by Wiener (1958), especially when dealing with biological objects. For a detailed discussion and outline of the theory see French (1976). One aim in using the approach proposed by French (1976) is to break down the system investigated into a series of simple systems, i.e., to localize certain filters (see e.g., French and Wong 1977). In the present work, however, we were interested in the amount of non-linearity of the sensory system as a whole.

The zero-order kernels measure the activity of sensory cells prior to stimulation. Usually, these cells are not spontaneously active. Perhaps, considering the high sensitivity of this sensory system (Tautz et al. 1981), small, undetected mechanical disturbances might have caused sufficient background activity to account for the observed positive value of K_0.

The first-order kernels express the probability of impulse discharge of the sensory cells at different stimulus frequencies (Fig. 3a, d).

The second-order kernels (Fig. 4a, b) may be understood by assuming that the receptor is receiving

a stimulus which is the sum of two sine waves ($\omega + \eta$). The amplitude of the output (impulses/s) at $\omega + \eta$ can be predicted from the height of the surface at the intersection of the two frequencies. For a linear system there is no "crosstalk" between the input frequencies, $\omega + \eta$, and therefore $K_2(\omega,\eta) = 0$ for all frequencies.

Comparing the data for the two types of hair shows a striking difference in the phase-curves of $K_1(\omega)$. The abrupt change in the phase curve of the feathered hairs below 20 Hz (Fig. 3b) is very similar to that found by French and Wong (1976) for tactile hairs in *Periplaneta americana,* in which this change occurs at around 8 Hz. In contrast, the smooth hairs (Fig. 3e) show a number of such abrupt phase changes, i.e., phase-locking is not observed for any stimulus-frequency range. This fact could be explained by the linearizing effect (Spekreijse and Oosting 1970) that can reduce strict phase coupling and which occurs as a consequence of noisy input to a system. If so, the smooth hairs would obviously be more sensitive to this effect than the feathered hairs.

Damped oscillations result in the time-domain representation (Fig. 3c, f). The negative values obtained could be taken as a suppression of impulse frequency. However, in other cases (e.g., horizontal cells: see Marmarelis and Naka 1973) this effect was interpreted on the basis of a feedback mechanism. For the mechanoreceptors reported here, feedback can be excluded since there is no known cross-coupling between receptor cells. However, threshold or adaptation effects that are dependent on stimulus frequency may be responsible for this result.

In natural situations, smooth hairs are displaced directly by water movement or touch, while feathered hairs are stimulated only indirectly, via bending of the antennal flagellum. The mechanical resonance of the flagellum is around 110 Hz in *Astacus leptodactylus* (Tautz et al. 1981), the frequency best transmitted by the feathered hairs to the sensory cells, as shown both by earlier threshold determinations (Tautz et al. 1981) and by the present investigation. The most sensitive frequencies for smooth and feathered hairs in *Astacus* (40 Hz and 90 Hz, respectively – Tautz et al. 1981) do not correspond exactly with the frequencies having the largest gain in *Orconectes* (60 Hz and 110 Hz, respectively). This slight discrepancy might be caused by the fact that the two investigations were done on different species of crayfish.

Where in the causal chain of events, which couple the stimulus to the generation of action potentials, the described non-linearities occur remains to be investigated.

One clear advantage of noise analysis over sinusoidal or step inputs is that it allows a complete description of the non-linearities of the system. A further advantage, one of great importance when biological systems are being tested, is that a noise experiment much better resembles a natural situation than do sinusoidal or step stimuli. Freshwater crayfish live in streams where turbulence produces complex mixture of stimulus frequencies that form the background from which crayfish have to distinguish behaviourally relevant signals.

Acknowledgements. We thank Drs. H. Markl, B. W. Ache and N. H. Fletcher for kindly reading drafts of the manuscript and R. Müller-Tautz for the drawings. Supported by a grant of the Ministry of Education of Japan to YE and the Deutsche Forschungsgemeinschaft, grant to JT (Ta 82/2-1).

References

Bender M, Gnatzy W, Tautz J (1984) The antennal feathered hairs in the crayfish: a non-innervated stimulus transmitting system. J Comp Physiol 154: 45–47

Chapman KM, Smith RS (1963) A linear transfer function underlying impulse frequency modulation in a cockroach mechanoreceptor. Nature 197: 699–700

French AS (1976) Practical nonlinear system analysis by Wiener kernel estimation in the frequency domain. Biol Cybernetics 24: 111–119

French AS, Butz EG (1973) Measuring the Wiener kernels of a nonlinear system using the fast Fourier transform. Int J Control 17: 529–539

French AS, Holden AV (1971) Alias-free sampling of neuronal spike trains. Kybernetik 8: 165–171

French AS, Wong RKS (1976) The response of trochanteral hair plate sensilla in the cockroach to periodic and random displacements. Biol Cybernetics 22: 33–38

French AS, Wong RKS (1977) Nonlinear analysis of sensory transduction in an insect mechanoreceptor. Biol Cybernetics 26: 231–240

Marmarelis PZ, Marmarelis VZ (1978) Analysis of physiological systems. The white noise approach. Plenum Press, New York

Marmarelis PZ, Naka KI (1973) Nonlinear analysis and synthesis of receptive-field response in the catfish retina. Part I: Horizontal cell – ganglion cell chain. J Neurophysiol 36: 605–618

Spekreijse H, Oosting H (1970) Linearizing: a method for analyzing and synthesizing nonlinear systems. Kybernetik 7: 22–31

Tautz J, Masters M, Aicher B, Markl H (1981) A new type of water vibration receptor on the crayfish antenna: I. Sensory physiology. J Comp Physiol 144: 533–541

Wiener N (1958) Nonlinear problems in random theory. John Wiley and Sons, New York